S-adenosylhomocysteine hydrolase inhibition by 3-deazaneplanocin A analogues induces anti-cancer effects in breast cancer cell lines and synergy with both histone deacetylase and HER2 inhibition

Annette Hayden, Peter W. M. Johnson, Graham Packham, Simon J. Crabb

S-adenosylhomocysteine hydrolase inhibition by 3-deazaneplanocin A analogues induces anti-cancer effects in breast cancer cell lines and synergy with both histone deacetylase and HER2 inhibition

Annette Hayden, Peter W.M. Johnson, Graham Packham and Simon J. Crabb*

Cancer Research UK Centre, University of Southampton School of Medicine, Southampton, United Kingdom

*Corresponding author: Dr Simon J. Crabb, Cancer Research UK Centre, University of Southampton School of Medicine, Mailpoint 824, Southampton General Hospital, Tremona Road, Southampton, United Kingdom, SO16 6YD. Email: S.J.Crabb@southampton.ac.uk. Phone: +44 (0)23 8079 5170. Fax: +44 (0)23 8079 5152

Abstract

Epigenetic abnormalities including abnormal histone methyltransferase activity contribute to breast cancer pathogenesis. An example is over expression of the polycomb repressive complex (PRC) 2 member enhancer of zeste homolog 2 (EZH2) which is linked to epigenetic silencing and poor prognosis. Recent evidence shows that S-adenosylhomocysteine (AdoHcy) hydrolase inhibitors (AHI) such as 3-deazaneplanocin A (DZNep) modulate chromatin through indirect inhibition of histone methyltransferases including EZH2. We investigated the biological effects of AdoHcy hydrolase inhibition using DZNep and its structural analogues 3-deazaadenosine (DZA) and neplanocin A (Nep A) in breast cancer cells. EZH2 protein expression was decreased and dose dependent growth inhibition occurred with variable potencies in MCF7, MDA-MB-231 and SKBr3 breast cancer cells. Cellular proliferation was inhibited through G_2/M cell cycle arrest and apoptosis. In addition breast cancer cells accumulated cytoplasmic lipid droplets in response to AdoHcy hydrolase inhibition consistent with a differentiating effect. Each analogue induced a similar pattern of biological activity against breast cancer cells but with differences in potency (DZA>DZNep>Nep A). Co-administration with the histone deacetylase (HDAC) inhibitor trichostatin A (TSA) induced synergistic inhibition of breast cancer cell proliferation. Furthermore the relatively AHI resistant human epidermal growth factor receptor 2 (HER2) positive cell line SKBr3 underwent synergistic growth inhibition in response to co-treatment with the HER2 directed therapeutic antibody trastuzumab. In conclusion, AHI induce growth inhibition, cell cycle arrest, apoptosis and differentiation in breast cancer cells and synergise with HDAC and HER2 inhibition. Targeting histone methyltransferase activity might be of therapeutic value in breast cancer.

Key words: S-adenosylhomocysteine hydrolase, 3-Deazaneplanocin A, histone deacetylase inhibitor, breast cancer, trastuzumab, enhancer of zeste homolog 2

Introduction

In addition to abnormalities of DNA sequence, epigenetic changes are also recognised to underpin breast cancer development. Such abnormalities are attractive for therapeutic intervention in that, unlike DNA sequence changes, they are potentially open to direct modulation through inhibition of enzymatic mediators [10, 31]. Abnormal epigenetic marks in breast cancer are described at the level of DNA methylation and post-translational modifications to histones. Histone acetylation is generally functions as a transcriptionally activating mark whilst DNA methylation at gene promoters produces repression. In contrast, histone methylation marks may be either repressive or activating dependent on the relevant lysine/arginine methylation site within the histone tail [10]. In addition to DNA methylation and histone acetylation, there is increasing evidence to implicate histone methylation as a potential therapeutic target for cancer. The main mediator of histone methylation studied to date in breast cancer is EZH2, a member of PRC2 which also includes embryonic ectoderm development (EED) and suppressor of zeste 12 homolog (SUZ12). EZH2 has a role in regulation of transcriptional regulation and chromatin state. PRC2 induces silencing initiation whilst a further complex, PRC1, with more variable composition including BMI1 and RING1b, allows for gene silencing maintenance. EZH2 is a histone methyltransferase which induces transcriptionally repressive trimethylation marks at histone H3 lysine 27 (H3K27me3) [18, 29]. Histone lysine methyltransferases such as EZH2 require methyl group donation from the cofactor S-adenosyl-L-methionine (AdoMet). EED and SUZ12 are required in complex for full functional activity. In addition, EZH2 induces transcriptional effects distinct from its histone methylation and methyltransferase activity, for example transcriptionally repressive or activating effects mediated through oestrogen and Wnt signalling pathways [15, 30, 32, 34]. EZH2/PRC2 activity occurs in concert with other transcriptionally repressive epigenetic processes. Thus histone methyltransferase activity of EZH2 is potentiated by the recruitment of HDAC activity through interaction with EED [35]. Furthermore, DNA methyltransferase binding to EZH2 repressed genes depends on the presence and activity of EZH2 which is required for DNA methylation of EZH2 target promoters [36].

EZH2 is over-expressed in breast cancer compared with normal breast epithelia and expression is associated with invasiveness, increased proliferation, markers of an aggressive phenotype (basal or HER2 positive) and reduced survival outcomes [1, 3, 6, 17, 28]. Overexpression of EZH2 in immortalized mammary epithelial cell lines promotes anchorage independent growth and cell invasion and EZH2 over-expressing cells are tumorigenic

when injected into mammary fat pads of nude mice [4, 17]. Furthermore EZH2 is required for embryonic stem cell survival and deletion is embryonic lethal [25]. EZH2 knockdown in oestrogen receptor negative cell line models decreased proliferation, inhibited G_2/M cell cycle transition and suppressed xenograft growth [12]. Therefore evidence for the role of EZH2 in breast cancer indicates a potential therapeutic target for the manipulation of epigenetic processes in breast cancer at the level of histone methylation. Furthermore, abnormal expression has been shown in breast cancer for other histone methyltransferases (e.g. NSD3 amplification, SMYD3 over-expression, PRMT1 depletion) along with over-expression of the histone demethylase JARID1B [21]. These are less well researched regarding relevance to breast cancer pathogenesis or potential therapeutic targets.

Recent evidence indicates that the carbocyclic adenosine analogue DZNep has anti-tumour activity which stems, at least in part, from PRC2 inhibition through decreased expression and activity of EZH2. DZNep inhibits AdoHcy hydrolase, preventing hydrolysis of AdoHcy to homocysteine and methionine. Subsequent cellular accumulation of AdoHcy results in upstream inhibition of AdoMet metabolism (to AdoHcy). AdoMet metabolism represents a key cellular mechanism for methyl group donation for a variety of dependant metabolic processes which are therefore disrupted, including production of methyltransferases such as EZH2.

DZNep and other AHI analogues have been previously investigated as potential anti viral agents [9]. In an initial report describing anticancer effects, DZNep induced depletion of EZH2, EED and SUZ12, and reversal of repressive H3K27me3 and H4K20me3 marks along with apoptosis in breast cancer (MCF7) and colorectal cancer cell line models. DZNep induced re-expression of a gene set with partial overlap to those re-expressed by siRNA depletion of PRC2 components. Precise mechanisms of EZH2 depletion by DZNep remain unclear but appear to be in part a function of proteasomal degradation and linked to dependency of PRC2 members on each other for stability and function [11, 27, 33]. Subsequent work has shown DZNep is in fact likely to have broader inhibitory effect on methyltransferases beyond EZH2. Indeed removal of both repressive (H3K27me3, H4K20me3) and activating (H3K4me3) but not all (H3K9me3, H3K36me3) histone methylation marks was demonstrated [20]. Thus DZNep likely acts as a broad methyltransferase inhibitor with effects on both inhibitory and activating histone methylation marks that might allow resetting of the epigenetic 'ground state' [20]. Differences have been seen in the patterns of activating trimethylation marks at H3K4 in response to DZNep which were depleted in HT29, SW480 (colorectal) and MCF7 (breast) cancer cell lines but increased in OCI-

AML3 and HCL-60 (acute myeloid leukaemia, AML) cells [11, 16, 20, 33]. Thus effects by this agent may be cancer and/or context specific.

Here we describe biological anti cancer effects of DZNep in multiple breast cancer cell lines and extend findings to other AHI structural analogues for the first time. In addition we have investigated interactions seen with potentially complementary epigenetic and targeted therapeutic approaches for breast cancer.

Methods

Cell Lines and Reagents

Reagents were from Sigma (Poole, UK) unless stated. MDA-MB-231, SKBr3, MCF10A and MCF7 cells (from ECACC, Salisbury, UK) were maintained in Dulbecco's modified Eagle's medium (Lonza, Wokingham, UK) with 10% (v/v) fetal calf serum (PAA Laboratories, Pasching, Austria), 2mM L-Glutamine and 5000 U/ml penicillin/streptomycin (Invitrogen, Paisley, UK) at 37°C with 10% (v/v) CO_2. Normal human dermal fibroblasts (NHDF) were maintained in Fibroblast Basal Medium with 10% (v/v) fetal calf serum and 0.5 mg/ml hydrocortisone (Cambrex, Wokingham, UK) at 37°C in 5% (v/v) CO_2. DZNep (NSC 606385), DZA (NSC 167897), and Nep A (NSC 316458) were obtained from the NCI/DTP Open Chemical Repository (http://dtp.cancer.gov) and kept as stock solutions in dimethyl sulfoxide (DMSO) at -20°C. Chemical structures are shown in Figure 1a. Trastuzumab was a kind gift from Southampton University Hospitals NHS Trust Pharmacy Department.

Immunoblotting

Cells were plated at $1.5x10^5$ per 35 mm well. After 24 hours, cells were treated by replacement of culture medium supplemented with the indicated compound or equivalent concentration of DMSO solvent. Samples were harvested as previously described for histone modifications [8] and for other proteins using detergent lysates [26]. Antibodies used were mouse monoclonal anti-EZH2 (3147) from New England BioLabs (UK) Ltd (Hitchin, UK), mouse monoclonal anti-HSC70 (sc-7298) and rabbit polyclonal anti-HER2 (sc-284) from Santa Cruz Biotechnology **(**Santa Cruz, CA) and rabbit polyclonal anti-H3K27me3 and rabbit polyclonal anti-acetylated histone H4 at lysine 8 (acH4K8) from Millipore (U.K.) Limited (Watford, UK). HSC70 expression was used as a protein loading control. Results are representative from a minimum of two separate experiments.

Cell Proliferation Assays

Cells (1000/well in a 96 well plate) were incubated for 6 days in various concentrations of compound or solvent control, prior to cell number analysis using MTS reagent (Promega, Southampton, UK) according to the manufacturer's instructions. 5 µL MTS reagent was added per well containing 100 µL of culture medium for 1.5 hours prior to colorimetric analysis on a Varioskan Flash spectral plate reader (Thermo Scientific, Basingstoke, UK). Each data point was derived from triplicate determinations and results are expressed as mean values as percentage MTS conversion with respect to samples exposed to DMSO solvent alone. (DMSO did not alter MTS conversion compared to untreated cells in any experiment, data not shown). IC_{50} values were derived following non linear regression using GraphPad Prism software (GraphPad Software, La Jolla, CA) and are presented as mean values ± SEM from a minimum of three separate experiments in each cell line for each compound. Synergism in cell proliferation assays, as a result of combination exposure to compounds, was assessed using fractional effect analyses using CalcuSyn software (version 2.0, Biosoft, Cambridge, UK) according to the manufacturer's instructions. This software produces a combination index (CI) value where a value of less than 1.0 indicates a synergistic interaction [5].

Cell Cycle Analysis

Cells were plated at $1.5x10^5$ per 35 mm well. At 24 hours, cells were treated by replacement of culture medium supplemented with the relevant AHI compound or equivalent concentration of DMSO solvent for the indicated durations. Cells were harvested and stained with propidium iodide (PI) for analysis of cell cycle phase and sub-G_1 fraction content using flow cytometry as previously described [7]. Data were analysed as the percentage of cells in the indicated cell cycle phase of total cells in cell cycle and for analyses of cells in the sub-G_0 fraction as the percentage of total cells. Presented data are a representative experiment from a minimum of 2 separate experiments in each indicated cell line. All experiments were performed with triplicate determinations for each data point.

Analysis of Apoptosis

Cells were plated at $1.5x10^5$ per 35 mm well. At 24 hours, cells were treated by replacement of culture medium supplemented with the indicated compound or equivalent concentration of DMSO. Cells were harvested after the durations indicated and flow cytometry was undertaken as previously described [7]. Cells were stained by

resuspending in 500 µL of binding buffer containing 2.5 µL of annexin V-FITC, 1.25 µL of PI or both per sample. Presented data are a representative experiment from a minimum of 2 separate experiments in each indicated cell line. All experiments were performed with triplicate determinations for each data point. Data are presented as the percentage of total cells that are either live (unstained), early apoptotic (annexin V positive) or late apoptotic (annexin V/PI positive).

Differentiation analysis

$1.5x10^5$ cells per 35 mm well were plated on pre-sterilised microscope slides. After 24 hours cells were treated with DZNep. Nile red staining for analysis of differentiation (of cytoplasmic lipid droplet accumulation) according to the methods of Greenspan et al [13], was carried out as previously described [7]. All data are representative from a minimum of 2 separate experiments. Presented data are a representative experiment from a minimum of 2 separate experiments in each indicated cell line. Lipid droplet quantification was undertaken in three separate reperasentative microspcope fields and a mean value per field of view ± SEM was determined.

Statistics

Determinations of statistically different mean values were performed using Students t-test.

Results

AHI analogues inhibit cell proliferation in breast cancer cells

Although previous reports show that DZNep can induce apoptosis in breast and other cancer cell lines [33], the structural analogues Nep A and DZA remain untested regarding their anticancer activity. We compared each in cell proliferation assays, revealing significant and consistent differences in potencies with respect to growth inhibition in each of three breast cancer cell lines (Fig. 1b-e). Using MCF7 cells as a reference, DZA is ~4 fold more potent then DZNep ($p \leq 0.01$) with both being nanomolar inhibitors of proliferation, and ~200 fold more potent compared to Nep A ($p \leq 0.05$). IC_{50} values for growth inhibition in MCF7 cells were DZA 55 ± 13 nM; DZNep 194 ± 20 nM; Nep A 11895 ± 2012 nM. Similar IC_{50} values and potencies were seen in MDA-MB-231 cells (DZA 57 ± 15 nM; DZNep 235 ± 26 nM; Nep A 11920 ± 1711 nM). SKBr3 cells exhibited relative resistance by ~2-4 fold for IC_{50} values of each compound compared to MCF7 cells (DZA 97 ± 11 nM; DZNep 821 ± 251 nM; Nep A 21225 ± 275 nM). DZNep did not induce a growth inhibitory effect in normal cells in concentrations up to 100 µM including non-cancerous breast epithelial cells (MCF10A) and NHDFs, therefore preferentially inhibiting cancer cell growth (Fig. 1f).

AdoHcy hydrolase inhibition induces G_2/M cell cycle arrest and apoptosis of breast cancer cell lines

Having shown that AHI analogues inhibit proliferation of breast cancer cells we investigated if this was due to cell cycle arrest and/or cell death. Time course experiments to determine cell cycle effects of DZNep were performed at a dose of 10µM as this was found to produce robust inhibition of cell proliferation (Fig. 2; Supplementary Table S1). DZNep induced cell cycle arrest and significant increase in the G_2/M cell component after 72 hours in MCF7 and MDA-MB-231 cells (Fig. 2b, c; Supplementary Table S1). SKBr3 cells remained relatively resistant to DZNep until 144 hours undergoing a more modest but statistically significant G_2/M arrest (Fig. 3d, Supplementary Table S1). DZNep also induced a significant increase in the sub-G_0 cell component (indicative of cell death) after 144 hours in each cell line (Fig. 2e, Supplementary Table S1). We also tested the effects of DZA on cell cycle progression and again found G_2/M cell cycle arrest and cell death after 72 hours in MCF7 cells (Fig. 2f, g, Supplementary Table S2).

Experiments to determine if cell death was occurring through induction of apoptosis revealed a significant increase in annexin V and annexin V/PI positive cells after 144 hours exposure to 10 μM DZNep in all three breast cancer cell lines (Fig. 3) indicating induction of apoptosis in response to AdoHcy hydrolase inhibition.

AdoHcy hydrolase inhibition induces cytoplasmic lipid accumulation in breast cancer cells

After 72 hours exposure to DZNep, MCF7 and MDA-MB-231 cells underwent morphological changes, increasing in size with a reduced nuclear to cytoplasmic ratio and lacking the regular uniform order of untreated cells. Changes in SKBr3 cells were less marked (Fig. 4a). Accumulation of cytoplasmic lipid droplets is validated as an experimental marker of cellular differentiation in breast cancer cells using methods described by Greenspan et al [7, 8, 13, 23]. We therefore undertook Nile red staining of cytoplasmic lipid droplets following DZNep exposure. This revealed significantly increased droplet numbers in all three cell lines although SKBr3 cells have higher background staining and a less marked increase compared to untreated cells (Fig. 4b, c). These results are consistent with a differentiation response to AdoHcy inhibition in breast cancer cells.

Combination AdoHcy hydrolase/HDAC inhibition has synergistic anti breast cancer effects

Combination epigenetic approaches are being investigated clinically and previous reports indicate synergistic interactions between HDAC inhibition and DZNep in AML and colorectal cancer models [11, 16, 24]. We therefore investigated for interactions between either DZNep or DZA and the pan zinc dependant (class I, II and IV) HDAC inhibitor TSA in breast cancer cell lines in growth inhibition assays. We found synergistic interaction with respect to growth inhibition between DZNep and TSA in MCF7 and MDA-MB-231 cells (Fig. 5a). At doses of 100 nM and 25 nM respectively for example, the individual drugs inhibited growth by less than 10% in MCF7 cells, compared to over 40% when the drugs are combined. In MCF7 and MDA-MB-231, cells evidence for a synergistic interaction was supported by detection of a CI value of less than 1.0. By contrast, DZNep and TSA were found to be additive (CI ≈ 1) rather than synergistic in SKBr3 cells. EZH2 expression and acH4K8 were assessed in cell lines treated with DZNep, TSA or both in all three cell lines (Fig. 5b). In each, EZH2 depletion and H4K8 hyperacetylation was detected in response to each agent individually which was greater with dual administration.

Combination growth inhibition assays were further explored using 25 nM DZA and 25 nM TSA (Fig. 5c). Significantly increased growth inhibition was observed in all cell lines with the combination treatment compared to either agent alone. Evidence for a synergistic interaction was supported by a CI value < 1.0 for each cell line. Immunoblot analysis demonstrated depletion of both EZH2 expression and H3K27 trimethylation to be enhanced in DZA and TSA dual treated cells (Fig. 5d).

Combined AdoHcy hydrolase/HER2 inhibition synergizes in HER2 over-expressing breast cancer cells

Our experiments found AHIs to be less potent against SKBr3 cells which are a model for HER2 over expressing breast cancer. We therefore hypothesized that combination therapy with the HER2 directed therapeutic monocolonal antibody trastuzumab might 'unlock' sensitivity to inhibitors of AdoHcy hydrolase. Combination growth inhibition assays were performed for AdoHcy hydrolase inhibition and trastuzumab in SKBr3 cells (Fig. 6a). More marked growth inhibition was observed with the combination treatment supported by a CI of 0.05 indicating strong synergism. Immunoblot analysis revealed a decrease in HER2 expression after either DZA or trastuzumab which was augmented by combination treatment (Fig. 6b).

Discussion

Recent data have shown EZH2 depletion and modification of histone methylation status by DZNep in MCF7 breast cancer cells [20, 33]. We sought to characterise the biological effects of this and other AHI compounds in model systems for this disease. Our results confirm the ability of DZNep to reduce expression of EZH2 in MCF7 cells but also now other breast cancer cell lines and to inhibit cell proliferation with nanomolar potency. Importantly, this anti-proliferative effect was not seen in two non-malignant cell line models. Thus, analogous to HDAC inhibition, AdoHcy hydrolase inhibition may provide an opportunity to target a therapeutic window between malignant and non-malignant cells by exploiting differing epigenetic profiles. However, the difference in potency ratio between malignant and non malignant models is markedly greater for AHIs than for HDAC inhibitors where ratios of 4-30 fold in potency are described [8, 14]. Our work therefore provides a rationale to target histone methylation dynamics in breast cancer.

For the first time, we have also demonstrated anti breast cancer effects for other AHIs using the DZNep structural analogues DZA and Nep A. Over 30 carbocyclic and acyclic adenosine analogue AHIs have been investigated for antiviral activity since the 1980s. Most exhibit broad antiviral activity which correlates to in vitro potency as AdoHcy hydrolase inhibitors [9]. As the mechanism of activity is through secondary inhibition of methyl donors from AdoMet, it is reasonable to assume that AdoMet dependant methyltransferase inhibition, and thus anticancer activity, represents a class effect. Differences in anti breast cancer cell potency occurred amongst the compounds we investigated (DZA>DZNep>Nep A). In contrast, from the antiviral literature, differing relative antiviral potencies (inhibition of cytopathogenicity in primary rabbit kidney cells against vaccinia or vesicular stomatitis viruses) were seen for these compounds (DZNep≈NepA>DZA) [9]. Factors underpinning potency differences as anti-cancer agents such as cellular uptake, intra cellular drug metabolism, AdoHcy hydrolase affinity, target specificity and drug efflux remain to be determined. Further investigation of the anti-cancer activity of this group of compounds is warranted and raises opportunities to begin to dissect structure/function relationships. Beyond this agent class, specific inhibitors of EZH2 and other methyltransferase enzymes would be of great interest. This would allow assessment of specificity of action on anti cancer activity in comparative studies to AHIs which appear likely to be indirect broad methyltransferase inhibitors [20]. As

with HDAC inhibition, it remains unclear whether target selectivity (e.g. for EZH2) will be valuable when developing a therapeutic approach based around histone methyltransferase activity.

Having demonstrated potent anti breast cancer effects of AHIs, we sought to describe the biological processes underpinning this. We have shown that both DZNep and DZA have multifactorial anticancer effects including induction of G_2/M cell cycle arrest, apoptosis and differentiation. Thus inhibition of AdoMet dependent methyltransferases by AHIs to reset epigenetic abnormalities in breast cancer mirrors biological effects produced by HDAC inhibition [8, 14]. We found such effects generally required 72 to 144 hours to become apparent at concentrations around the IC_{50} value for growth inhibition in contrast to HDAC inhibition which in our experience is more rapid in its biological action (typically 24 to 72 hours) [8]. This may have implications if such compounds were developed towards clinical applications in terms of duration of exposure required for biological effect. This prolonged delay to biological outcome is also notable in light of recent data indicating that the epigenetic 'ground state' may rapidly reset (at least at the level of gene expression) following removal of DZNep [20].

We have also demonstrated synergistic interactions between AHIs and HDAC inhibition mirroring recent description of similar interactions in acute myeloid leukaemia and colorectal cancer models [11, 16]. Clinical evidence for efficacy of HDAC inhibition as a single agent approach in breast cancer has been modest to date and we and others have argued that HDAC inhibition will require a combination therapeutic strategy for optimal outcomes [19, 22, 24]. Our results are consistent with a model whereby optimal anti breast cancer effect is dependent on a more profound reset of underlying epigenetic abnormalities requiring both HDAC and histone methyltransferase inhibition. PRC2 recruitment of HDACs by EED to augment transcriptional repression might potentially underpin the mechanism by which such synergy occurs [35]. Such combination strategies should therefore be investigated further for this disease as well as combinations with DNA methyltransferase inhibition in view of the recruitment of DNA methyltransferase activity to H3K27me3 repressive marks by EZH2 [36].

In addition, we have demonstrated synergistic interaction between AHIs and trastuzumab in a HER2 over expressing breast cancer model. This was accompanied by a reduction in HER2 protein expression which was maximised by co-administration. Mechanisms for HER2 depletion remain to be elucidated but might include effects on transcription through chromatin remodelling or indirectly for example by interacting with chaperone

(e.g. HSP90) function as is seen with HDAC inhibition [2]. Therapeutic targeting of histone methylation status in combination with established anti HER2 targeted therapies may therefore be of value in breast cancer subtypes dependant on this pathway. The mechanistic interaction between these two therapeutic approaches warrants further investigation.

In conclusion, we have demonstrated that the anti-breast cancer effects of AdoHcy hydrolase inhibition are underpinned by G_2/M cell cycle arrest, apoptosis and cellular differentiation and that these are class effects for AHI analogues. Furthermore, AHIs produce synergistic interactions with HDAC inhibition and HER2 targeted therapy in breast cancer models. Our findings provide a basis for the development of therapeutic strategies to target histone methylation profiles in breast cancer.

Acknowledgements

This work was supported by Cancer Research UK and Wessex Medical Research.

References

1. Bachmann IM, Halvorsen OJ, Collett K, Stefansson IM, Straume O, Haukaas SA, Salvesen HB, Otte AP, Akslen LA (2006) EZH2 Expression Is Associated With High Proliferation Rate and Aggressive Tumor Subgroups in Cutaneous Melanoma and Cancers of the Endometrium, Prostate, and Breast. J Clin Oncol 24:268-273
2. Bali P, Pranpat M, Swaby R, Fiskus W, Yamaguchi H, Balasis M, Rocha K, Wang HG, Richon V, Bhalla K (2005) Activity of suberoylanilide hydroxamic Acid against human breast cancer cells with amplification of her-2. Clin Cancer Res 11:6382-6389
3. Bracken AP, Pasini D, Capra M, Prosperini E, Colli E, Helin K (2003) EZH2 is downstream of the pRB-E2F pathway, essential for proliferation and amplified in cancer. EMBO J 22:5323-5335
4. Cha T-L, Zhou BP, Xia W, Wu Y, Yang C-C, Chen C-T, Ping B, Otte AP, Hung M-C (2005) Akt-Mediated Phosphorylation of EZH2 Suppresses Methylation of Lysine 27 in Histone H3. Science 310:306-310
5. Chou TC (2010) Drug combination studies and their synergy quantification using the Chou-Talalay method. Cancer Res 70:440-446
6. Collett K, Eide GE, Arnes J, Stefansson IM, Eide J, Braaten A, Aas T, Otte AP, Akslen LA (2006) Expression of Enhancer of Zeste Homologue 2 Is Significantly Associated with Increased Tumor Cell Proliferation and Is a Marker of Aggressive Breast Cancer. Clin Cancer Res 12:1168-1174
7. Crabb SJ, Hague A, Johnson PW, Packham G (2008) BAG-1 inhibits PPARgamma-induced cell death, but not PPARgamma-induced transcription, cell cycle arrest or differentiation in breast cancer cells. Oncol Rep 19:689-696
8. Crabb SJ, Howell M, Rogers H, Ishfaq M, Yurek-George A, Carey K, Pickering BM, East P, Mitter R, Maeda S, Johnson PW, Townsend P, Shin-ya K, Yoshida M, Ganesan A, Packham G (2008) Characterisation of the in vitro activity of the depsipeptide histone deacetylase inhibitor spiruchostatin A. Biochem Pharmacol 76:463-475
9. De Clercq E (2005) John Montgomery's legacy: carbocyclic adenosine analogues as SAH hydrolase inhibitors with broad-spectrum antiviral activity. Nucleosides Nucleotides Nucleic Acids 24:1395-1415
10. Esteller M (2008) Epigenetics in cancer. N Engl J Med 358:1148-1159

11. Fiskus W, Wang Y, Sreekumar A, Buckley KM, Shi H, Jillella A, Ustun C, Rao R, Fernandez P, Chen J, Balusu R, Koul S, Atadja P, Marquez VE, Bhalla KN (2009) Combined epigenetic therapy with the histone methyltransferase EZH2 inhibitor 3-deazaneplanocin A and the histone deacetylase inhibitor panobinostat against human AML cells. Blood 114:2733-2743

12. Gonzalez ME, Li X, Toy K, DuPrie M, Ventura AC, Banerjee M, Ljungman M, Merajver SD, Kleer CG (2009) Downregulation of EZH2 decreases growth of estrogen receptor-negative invasive breast carcinoma and requires BRCA1. Oncogene 28:843-853

13. Greenspan P, Mayer EP, Fowler SD (1985) Nile red: a selective fluorescent stain for intracellular lipid droplets. J Cell Biol 100:965-973

14. Huang L, Pardee AB (2000) Suberoylanilide hydroxamic acid as a potential therapeutic agent for human breast cancer treatment. Mol Med 6:849-866

15. Hwang C, Giri VN, Wilkinson JC, Wright CW, Wilkinson AS, Cooney KA, Duckett CS (2008) EZH2 regulates the transcription of estrogen-responsive genes through association with REA, an estrogen receptor corepressor. Breast Cancer Res Treat 107:235-242

16. Jiang X, Tan J, Li J, Kivimae S, Yang X, Zhuang L, Lee PL, Chan MT, Stanton LW, Liu ET, Cheyette BN, Yu Q (2008) DACT3 is an epigenetic regulator of Wnt/beta-catenin signaling in colorectal cancer and is a therapeutic target of histone modifications. Cancer Cell 13:529-541

17. Kleer CG, Cao Q, Varambally S, Shen R, Ota I, Tomlins SA, Ghosh D, Sewalt RG, Otte AP, Hayes DF, Sabel MS, Livant D, Weiss SJ, Rubin MA, Chinnaiyan AM (2003) EZH2 is a marker of aggressive breast cancer and promotes neoplastic transformation of breast epithelial cells. Proc Natl Acad Sci U S A 100:11606-11611

18. Laible G, Wolf A, Dorn R, Reuter G, Nislow C, Lebersorger A, Popkin D, Pillus L, Jenuwein T (1997) Mammalian homologues of the Polycomb-group gene Enhancer of zeste mediate gene silencing in Drosophila heterochromatin and at S. cerevisiae telomeres. EMBO J 16:3219-3232

19. Luu TH, Morgan RJ, Leong L, Lim D, McNamara M, Portnow J, Frankel P, Smith DD, Doroshow JH, Gandara DR, Aparicio A, Somlo G, Wong C (2008) A Phase II Trial of Vorinostat (Suberoylanilide Hydroxamic Acid) in Metastatic Breast Cancer: A California Cancer Consortium Study. Clin Cancer Res 14:7138-7142

20. Miranda TB, Cortez CC, Yoo CB, Liang G, Abe M, Kelly TK, Marquez VE, Jones PA (2009) DZNep is a global histone methylation inhibitor that reactivates developmental genes not silenced by DNA methylation. Mol Cancer Ther 8:1579-1588

21. Miremadi A, Oestergaard MZ, Pharoah PD, Caldas C (2007) Cancer genetics of epigenetic genes. Hum Mol Genet 16 Spec No 1:R28-49

22. Munster P, Marchion D, Bicaku E, Lacevic M, Kim J, Centeno B, Daud A, Neuger A, Minton S, Sullivan D (2009) Clinical and biological effects of valproic acid as a histone deacetylase inhibitor on tumor and surrogate tissues: phase I/II trial of valproic acid and epirubicin/FEC. Clin Cancer Res 15:2488-2496

23. Munster PN, Troso-Sandoval T, Rosen N, Rifkind R, Marks PA, Richon VM (2001) The histone deacetylase inhibitor suberoylanilide hydroxamic acid induces differentiation of human breast cancer cells. Cancer Res 61:8492-8497

24. Nolan L, Johnson PW, Ganesan A, Packham G, Crabb SJ (2008) Will histone deacetylase inhibitors require combination with other agents to fulfil their therapeutic potential? Br J Cancer 99:689-694

25. O'Carroll D, Erhardt S, Pagani M, Barton SC, Surani MA, Jenuwein T (2001) The polycomb-group gene Ezh2 is required for early mouse development. Mol Cell Biol 21:4330-4336

26. Packham G, Brimmell M, Cleveland JL (1997) Mammalian cells express two differently localized Bag-1 isoforms generated by alternative translation initiation. Biochem J 328 (Pt 3):807-813

27. Pasini D, Bracken AP, Jensen MR, Lazzerini Denchi E, Helin K (2004) Suz12 is essential for mouse development and for EZH2 histone methyltransferase activity. EMBO J 23:4061-4071

28. Pietersen AM, Horlings HM, Hauptmann M, Langerod A, Ajouaou A, Cornelissen-Steijger P, Wessels LF, Jonkers J, van de Vijver MJ, van Lohuizen M (2008) EZH2 and BMI1 inversely correlate with prognosis and TP53 mutation in breast cancer. Breast Cancer Res 10:R109

29. Satijn DPE, Otte AP (1999) Polycomb group protein complexes: do different complexes regulate distinct target genes? Biochimica et Biophysica Acta (BBA) - Gene Structure and Expression 1447:1-16

30. Shi B, Liang J, Yang X, Wang Y, Zhao Y, Wu H, Sun L, Zhang Y, Chen Y, Li R, Zhang Y, Hong M, Shang Y (2007) Integration of Estrogen and Wnt Signaling Circuits by the Polycomb Group Protein EZH2 in Breast Cancer Cells. Mol. Cell. Biol. 27:5105-5119

31. Simon JA, Lange CA (2008) Roles of the EZH2 histone methyltransferase in cancer epigenetics. Mutation Research/Fundamental and Molecular Mechanisms of Mutagenesis 647:21-29

32. Su Ih, Dobenecker M-W, Dickinson E, Oser M, Basavaraj A, Marqueron R, Viale A, Reinberg D, Wülfing C, Tarakhovsky A (2005) Polycomb Group Protein Ezh2 Controls Actin Polymerization and Cell Signaling. Cell 121:425-436

33. Tan J, Yang X, Zhuang L, Jiang X, Chen W, Lee PL, Karuturi RK, Tan PB, Liu ET, Yu Q (2007) Pharmacologic disruption of Polycomb-repressive complex 2-mediated gene repression selectively induces apoptosis in cancer cells. Genes Dev 21:1050-1063

34. Tonini T, Bagella L, D'Andrilli G, Claudio PP, Giordano A (2004) Ezh2 reduces the ability of HDAC1-dependent pRb2//p130 transcriptional repression of cyclin A. Oncogene 23:4930-4937

35. van der Vlag J, Otte AP (1999) Transcriptional repression mediated by the human polycomb-group protein EED involves histone deacetylation. Nat Genet 23:474-478

36. Vire E, Brenner C, Deplus R, Blanchon L, Fraga M, Didelot C, Morey L, Van Eynde A, Bernard D, Vanderwinden JM, Bollen M, Esteller M, Di Croce L, de Launoit Y, Fuks F (2006) The Polycomb group protein EZH2 directly controls DNA methylation. Nature 439:871-874

Figure Legends

Fig. 1 AHI analogues inhibit breast cancer cell proliferation. (a), AHI chemical structures. (b), Mean IC_{50} values in breast cancer cell lines for DZA (open bars), DZNep (black bars) and Nep A (hatched bars). (c-e), Representative cell proliferation assays are shown for (c) MCF7, (d) MDA-MB-231 and (e) SKBr3 cells treated for 6 days with DZA (▼), DZNep (■) or Nep A (▲). (f), Representative cell proliferation assay in MCF10A (■) and NHDF (▲) cells following exposure to DZNep.

Fig. 2 AHIs induce G_2/M cell cycle arrest in breast cancer cell lines. (a), Representative flow cytometry histograms for PI stained MCF7 cells treated with 10 μM DZNep or DMSO solvent control. (b-d), bar charts representing percentages of cells in the indicated cell cycle phases, following treatment with 10 μM DZNep (black bars) or DMSO solvent control (open bars) in (b) MCF7, (c) MDA-MB-231 or (d) SKBr3 cells. (e), bar chart representing percentages of cells in the sub-G_0 fraction following treatment with 10 μM DZNep (black bars) or DMSO solvent control (open bars) in the indicated cell lines. (f), bar chart representing percentages of cells in the indicated cell cycle phases, following treatment with 10 μM DZA (black bars) or DMSO solvent control (open bars) in MCF7 cells. (g), bar chart representing percentages of cells in the sub-G_0 fraction following treatment with 10 μM DZA (black bars) or DMSO solvent control (open bars) in MCF7 cells. Bar charts show mean values from triplicate determinations in a representative experiment for each indicated cell line. * $p<0.05$, ** $p<0.01$ compared to DMSO control samples.

Fig. 3 AHIs induce apoptosis in breast cancer cell lines. (a), Representative flow cytometry raw data of FITC-annexin V (FL1) and/or PI (FL2) stained MCF7 cells treated with 10 μM DZNep or DMSO solvent control for 144 hours. (b-d), Apoptosis analysis of (b) MCF7, (c) MDA-MB-231 or (d) SKBr3 breast cancer cells treated with 10 μM DZNep (black bars) or DMSO solvent control (open bars). Q1, annexin V negative/PI negative; Q2, annexin V positive/PI negative; Q3, annexin V positive/PI positive; Q4, annexin V negative/PI positive. * $p<0.05$, ** $p<0.01$ compared to DMSO control samples.

Fig. 4 DZNep induces cytoplasmic lipid droplet accumulation in breast cancer cell lines. (a), Representative brightfield images comparing morphology of the indicated breast cancer cell lines exposed for 72 hours to 10 μM DZNep or DMSO. (b), Representative fluorescence microscopy images for Nile red staining of cytoplasmic lipid droplets of cells exposed for 72 hours to 10 μM DZNep or DMSO. (c), Histogram of quantified Nile red staining. Black bars, DZNep; white bars, DMSO control. Data represent the mean number ± SEM of lipid droplets per field of view. * $p<0.05$, ** $p<0.01$ compared to DMSO control samples.

Fig. 5 AdoHcy and HDAC inhibitors have synergistic effects in breast cancer cell lines. (a, c), histograms representing percentage inhibition in cell proliferation assays in the indicated cell lines compared to DMSO exposed cells (open bars) following exposure to (a) 100 nM DZNep (black bars), 25 nM TSA (diagonal hatched bars) or DZNep and TSA (horizontal hatched bars) or (c) 25 nM DZA (black bars), 25 nM TSA (diagonal hatched bars) or DZA and TSA (horizontal hatched bars). Data are mean ± SEM of triplicate determinations from a representative experiment . Synergistic effects on cell proliferation are indicated by CI values < 1.0. (b) and (d), Representative immunoblots to show expression of EZH2, acetylation of histone H4 at lysine 8 and trimethylation of histone H3 at lysine 27. Cells were exposed for 48 hours to DZNep or DZA followed by the addition or not of TSA for 24 hours as indicated. All experiments were performed a minimum of twice.

Fig 6 AdoHcy inhibition and trastuzumab have synergistic effects in HER2 over-expressing breast cancer cells. (a), Histogram representing percentage inhibition in cell proliferation assays following individual or combination exposure to 25 nM DZA and 1250 nM trastuzumab in SKBr3 cells. Data represents the percentage inhibition of cell proliferation compared to cells exposed to DMSO solvent alone. Data are mean ± SEM of triplicate determinations from a representative experiment. Synergistic effects on cell proliferation are indicated by a CI value < 1.0. (b), Representative immunoblot to demonstrate expression of HER2 at 48 hours following exposure to trastuzumab or DZA or both. All experiments were performed a minimum of twice.

Supplementary Tables

Supplementary Table S1 Cell cycle analysis of breast cancer cell lines in response to 10µM DZNep or DMSO solvent control

Cell line	Cell cycle phase	72 hours		144 hours	
		DMSO	DZNep	DMSO	DZNep
MCF7	Sub G_0	9.8 +/- 3.8	16.5 +/- 4.5	19.5 +/- 3.0	53.5 +/- 3.0
	G_1/G_0	74.5 +/- 2.0	54.0 +/- 2.5	74.3 +/- 0.8	51.3 +/-3.8
	S phase	6.5 +/- 1.0	7.0 +/- 0	5.3 +/- 0.8	8.3 +/-1.8
	G_2/M	17.5 +/- 1.0	38.3 +/- 3.3	20.0 +/- 2.5	40.3 +/- 1.8
MDA-MB-231	Sub G_0	4.0 +/- 0	10.17 +/- 1.3	6.5 +/- 0.8	46.83 +/- 9.2
	G_1/G_0	61.0 +/- 3.1	53.3 +/- 3.6	66.2 +/- 1.9	52.67 +/- 2.4
	S phase	14.4 +/- 1.2	14.2 +/- 1.3	11.0 +/- 0.6	15.34 +/- 0.9
	G_2/M	25.0 +/- 2.6	31.8 +/- 2.1	22.7 +/- 1.6	31.8 +/- 3.4
SKBr3	Sub G_0	9.0 +/- 0	14.0 +/- 0	17.5 +/- 0.7	38.0 +/- 1.4
	G_1/G_0	68.0 +/- 0	73.5 +/- 0.7	81.0 +/- 0	74.5 +/- 0.7
	S phase	9.5 +/- 0.7	7.0 +/- 0	5.0 +/- 0	6.5 +/- 0.7
	G_2/M	20.5 +/- 0.7	19.5 +/- 0.7	13.0 +/- 0	19.0 +/- 1.4

Results are presented as mean percentage of cells +/- SEM of cells in the indicated cycle phase of total cells in cycle or as mean percentage of total cells in the sub-G_0 (dead) cell fraction of total cells.

Supplementary Table S2 Cell cycle analysis of MCF7 breast cancer cell lines in response to 10μM DZA

Cell line	Cell cycle phase	72 hours	
		DMSO	DZA
MCF7	Sub G_0	13.5 +/- 0.5	27.0 +/- 0
	G_1/G_0	72.5 +/- 0.5	42.5 +/- 0.5
	S phase	4.5 +/- 0.5	14.5 +/- 0.5
	G_2/M	20.0 +/- 0	43.0 +/- 0

Results are presented as mean percentage of cells +/- SEM of cells in the indicated cycle phase of total cells in cycle or as mean percentage of total cells in the sub-G_0 (dead) cell fraction of total cells.

Figure
Click here to download high resolution image

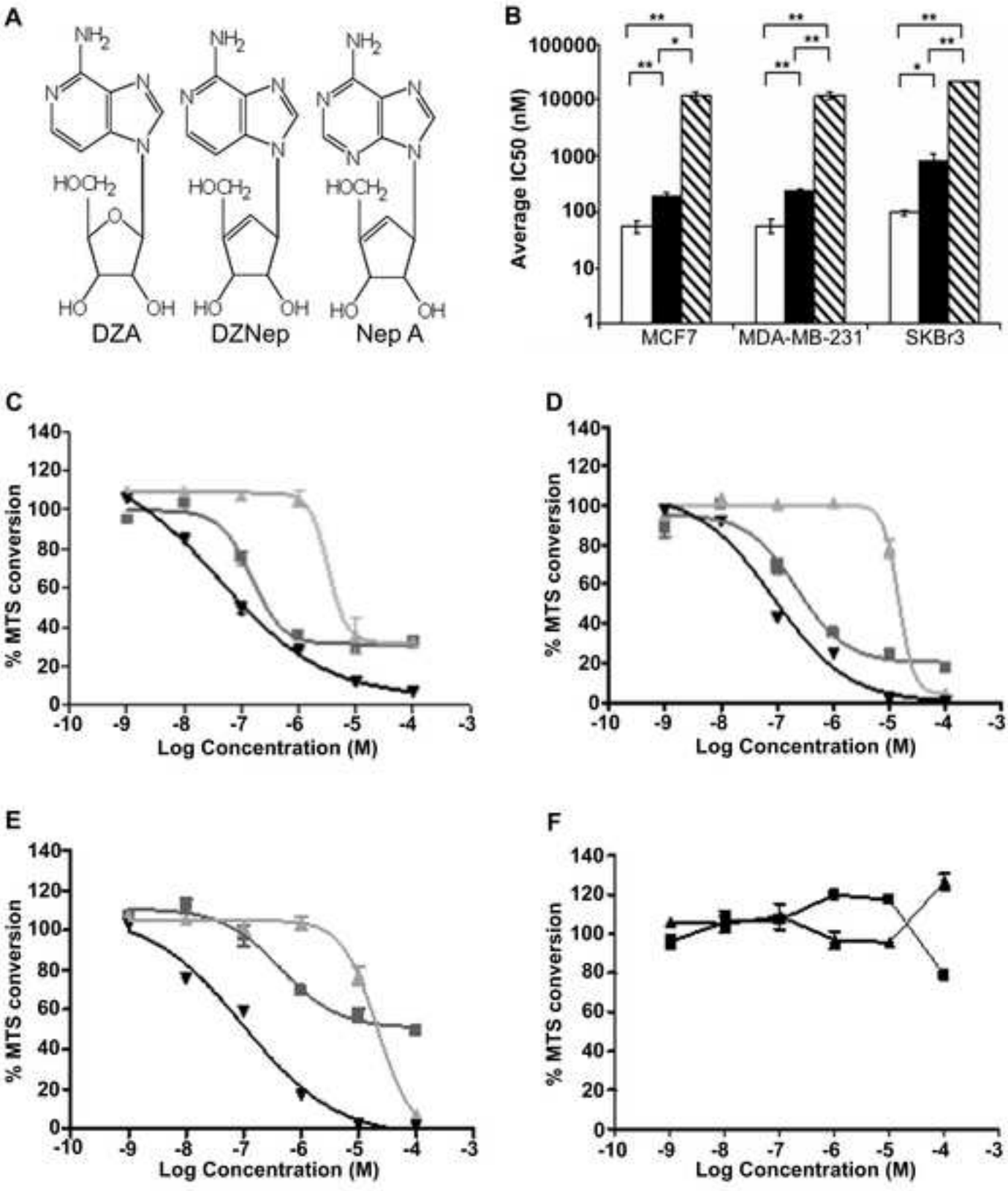

Figure 1

Hayden et al

Figure

Click here to download high resolution image

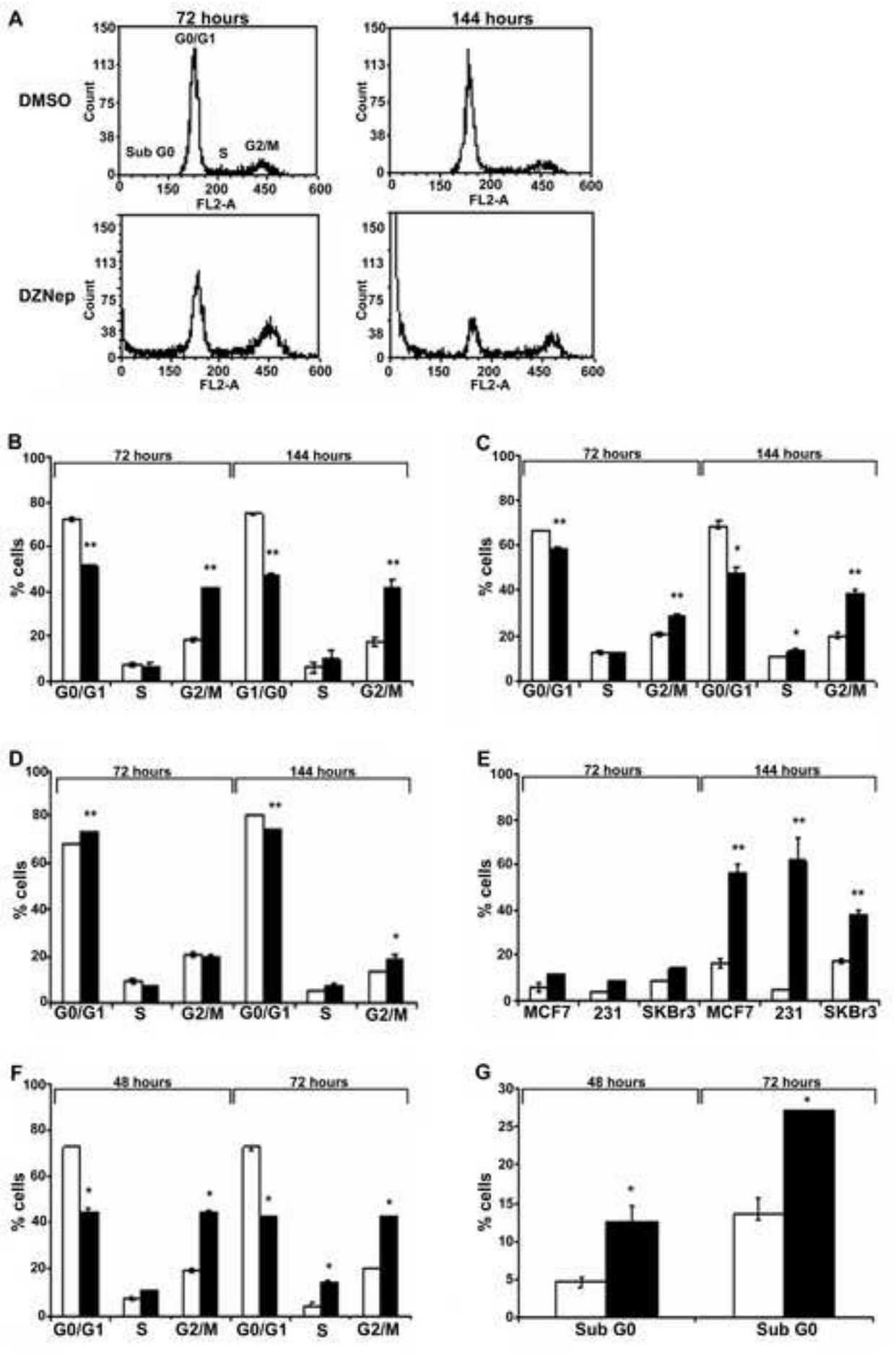

Figure 2

Hayden et al

Figure
Click here to download high resolution image

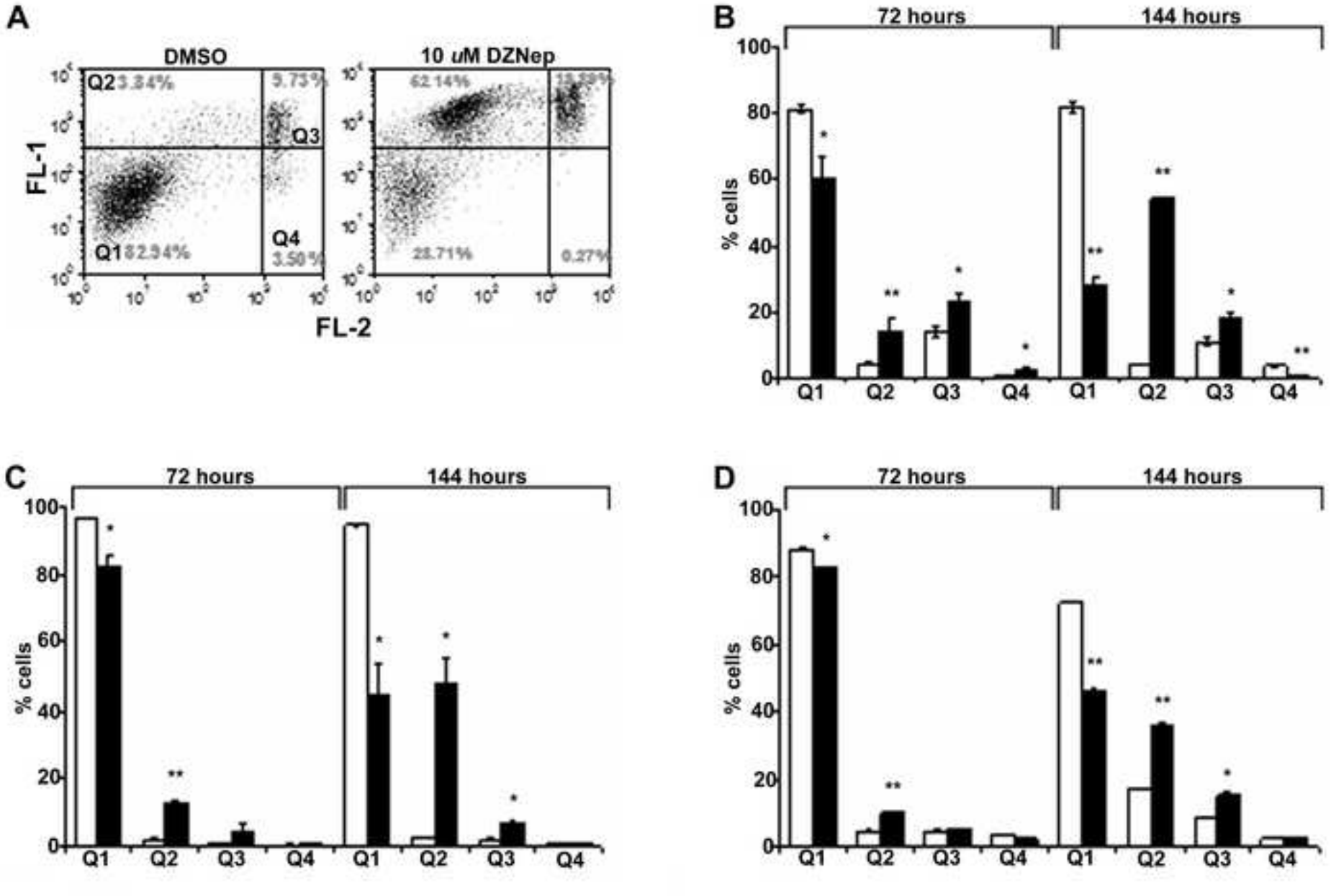

Figure 3 Hayden et al

Figure
Click here to download high resolution image

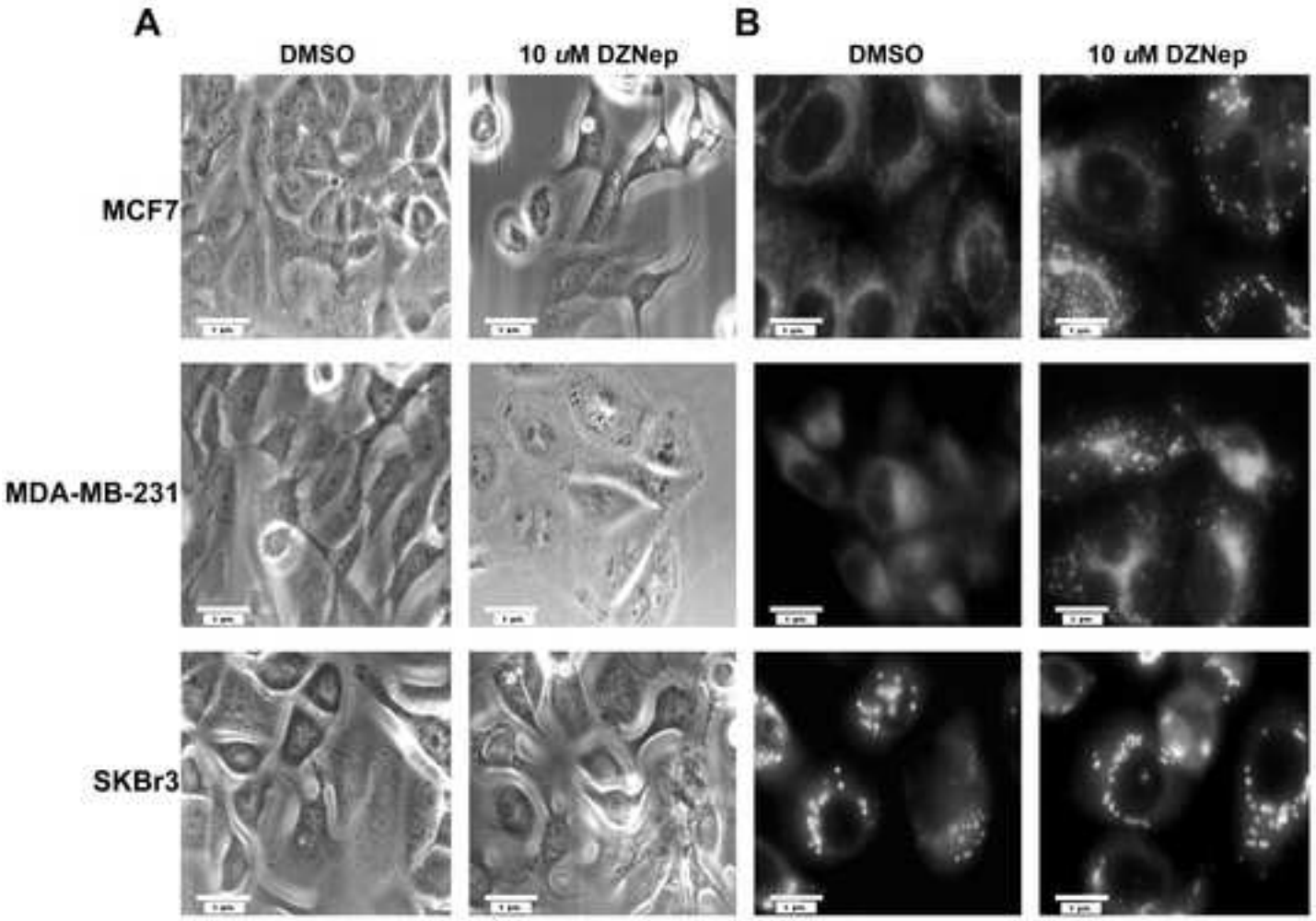

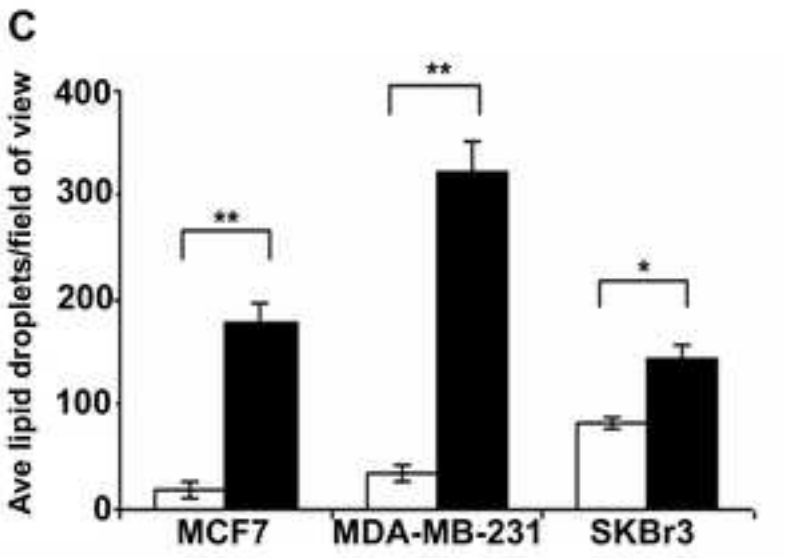

Figure 4
Hayden et al

Figure

Click here to download high resolution image

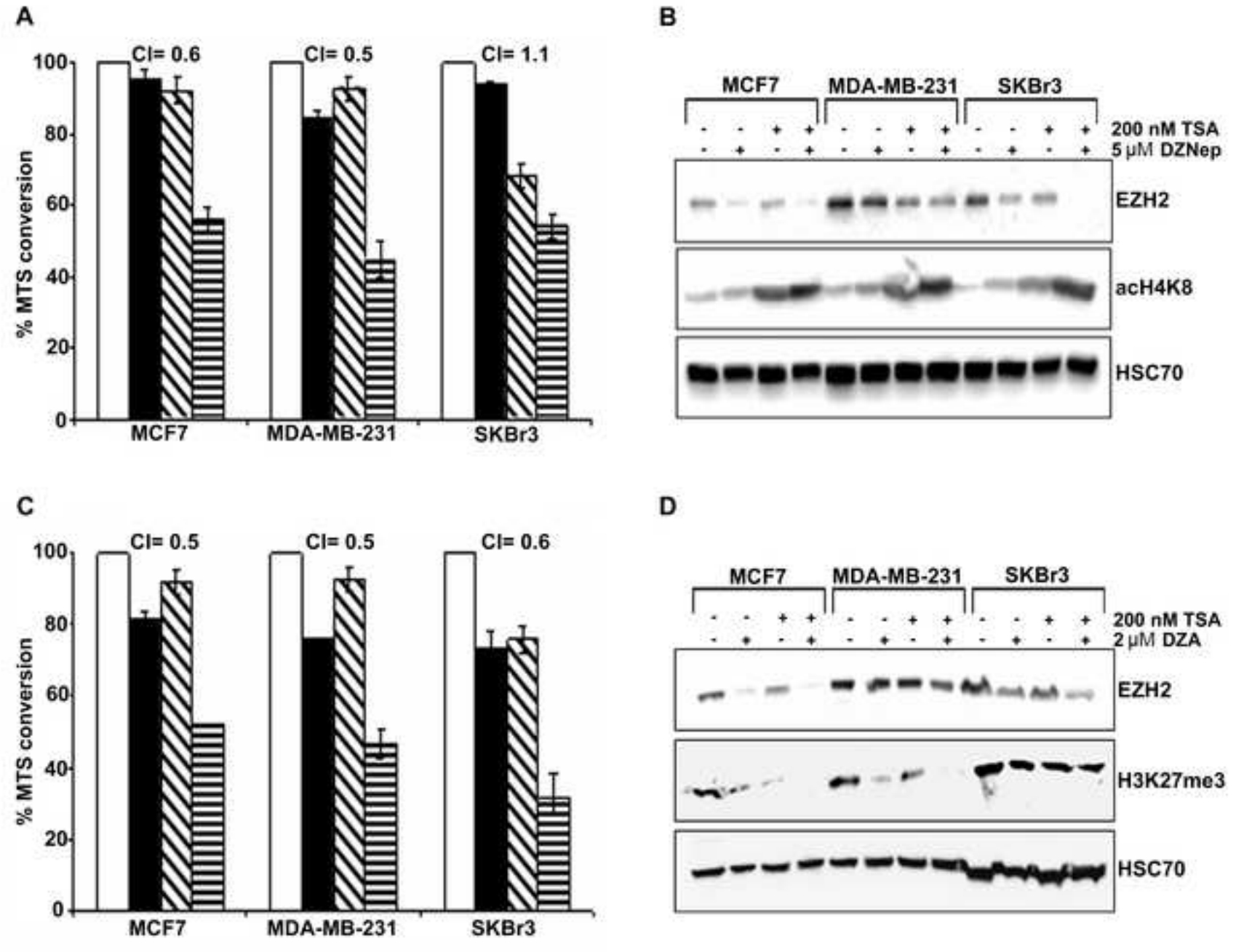

Figure 5

Hayden et al

Figure
Click here to download high resolution image

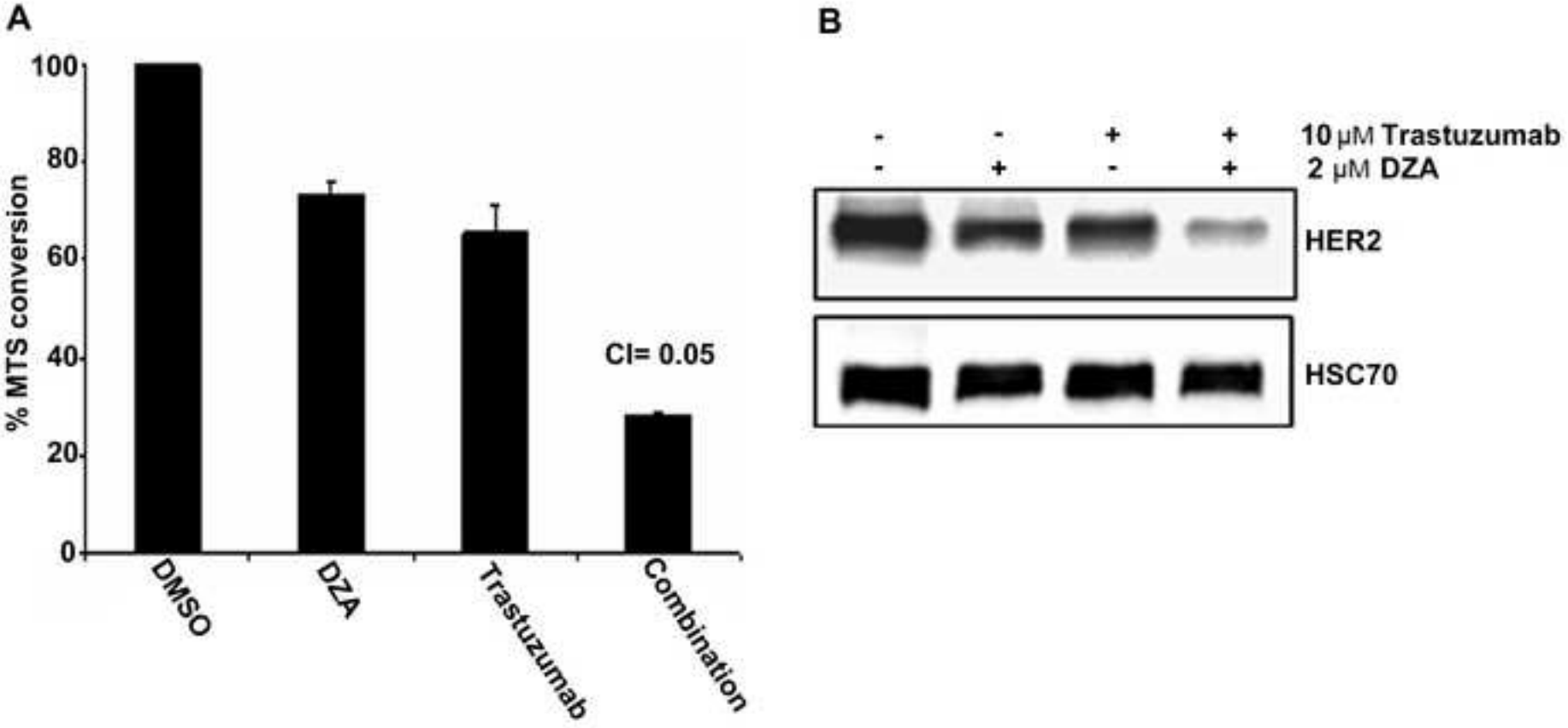

Figure 6 Hayden et al